Hydrogen Storage in Ni Nanoparticle-Dispersed Multiwalled Carbon Nanotubes

Hyun-Seok Kim,[†] Ho Lee,[‡] Kyu-Sung Han,[†] Jin-Ho Kim,[§] Min-Sang Song,[†] Min-Sik Park,[†] Jai-Young Lee,[†] and Jeung-Ku Kang*,[†]

Department of Materials Science and Engineering, Korea Advanced Institute of Science and Technology, 373-1 Guseong-dong, Yuseong-gu, Daejeon, South Korea, Samsung Electronics Co. Ltd., San 24, Giheung, Yongin, South Korea, and Samsung Advanced Institute of Technology, San 24, Giheung, Yongin, South Korea

Received: November 18, 2004; In Final Form: January 28, 2005

Hydrogen storage properties of mutiwalled carbon nanotubes (MWCNTs) with Ni nanoparticles were investigated. The metal nanoparticles were dispersed on MWCNTs surfaces using an incipient wetness impregnation procedure. Ni catalysts have been known to effectively dissociate hydrogen molecules in gas phase, providing atomic hydrogen possible to form chemical bonding with the surfaces of MWCNTs. Hydrogen desorption spectra of MWCNTs with 6 wt % of Ni nanoparticles showed that ∼2.8 wt % hydrogen was released in the range of 340−520 K. In Kissinger's plot to evaluate the nature of interaction between hydrogen and MWCNTs with Ni nanoparticles, the hydrogen desorption activation energy was measured to be as high as ∼31 kJ/mol·H_2, which is much higher than the estimates of pristine SWNTs. C−H_n stretching vibrations after hydrogenation in FTIR further supported that hydrogen molecules were dissociated when bound to the surfaces of MWCNTs. During cyclic hydrogen absorption/desorption, there was observed no significant decay in hydrogen desorption amount. The hydrogen chemisorption process facilitated by Ni nanopaticles could be suggested as an effective reversible hydrogen storage method.

Since discovery of carbon nanotubes (CNTs) in 1991 by Iijima,[1] hydrogen storage in CNTs has shown great promise as a high-energy density absorbent.[2,3] In many theoretical and empirical results, superior hydrogen gas absorbing property has been reported under a high pressure and often at an extremely low temperature.[4−7] The interaction mechanism between carbon and hydrogen has been attributed to physisorption of molecular hydrogen inside the tubes and interstitial sites in tube bundles.[4−7,16] Recently, studies on hydrogenation under a high pressure and at an elevated temperature have shown the possibility that every carbon atom on CNTs could be a potential site for chemisorption of one hydrogen atom.[8−10] Since it needs ∼440 kJ/mol·H_2 to break H−H bond of H_2 molecules, the chemical adsorption is unlikely to occur in gas phase except for these special environments. Experimentally, the doping of dissociative catalysts such as alkali metals has also activated the chemical adsorption process, resulting in much higher hydrogen storage capacity than that for the physisorption mechanism.[11,12] However, these alkaline dopants have higher hydrogen affinity and lower hydrogen molecules dissociative activity than transition metals such as Ni, Co, and Pt. Accordingly, it was difficult to conclude which was responsible for the improved storage capacity. For the better understanding of the role of dopants, it is necessary to investigate the relationship between hydrogen storage properties and the hydrogen molecules dissociative catalysts.

In this paper, we selected Ni as a dissociative catalyst for hydrogen and employed the incipient wetness impregnation method, which enabled nanosized catalysts to be dispersed on the carbon surface.[13,14] The hydrogen storage properties were determined by evolution temperature and quantity measured by thermal desorption spectrum (TDS) analysis. We also evaluated the possibility of chemical adsorption process assisted by Ni nanoparticles present on nanotube surface.

The MWCNTs were synthesized with microwave plasma enhanced CVD as presented in our previous works.[15,16] First, a cobalt layer with a thickness of 50 nm was deposited on p-type Si-substrate by rf magnetron sputtering at 100 W rf power and the pressure was adjusted to 30 mTorr by feeding Ar gas. Prior to the growth of CNTs in microwave PECVD, hydrogen was introduced and plasma treatment was conducted at 1100 W microwave power for 90 s. The plasma-treated cobalt seeds were used as catalytic seeds for the growth of MWCNTs. A mixture of H_2 (89.9%, vol %), CH_4 (0.1%), and O_2 (10%) was used as the gas source. The microwave power and working pressure during the growth of CNTs were 700 W and 30 Torr, respectively. The growth temperature was maintained at 750 °C using halogen lamp heating. No further process was performed to purify the soot or to open the tube end with as-produced samples. 0.005 g of MWCNTs was impregnated with 5, 10, 21, and 73 mM Ni nitrate acetone solutions of 10 mL. The metal loading amount was determined by concentration of the solution as reported by Joo et al.[14] After immersion, the black sample was dried in 60 °C and subsequently heat-treated in H_2 gas flow. To observe the hydrogen storage properties, hydrogen (99.999%) was charged under 4 MPa at 300 K for 2 h in 0.002 g MWCNTs with nanoparticle dispersion. The sample was placed in a quartz reactor, which was surrounded by liquid nitrogen cooled cryostat and wound by heating element with a programmable power supply. The injection port of gas chromatograph was connected directly to the reactor and high-purity Ar (99.999%) of 1 atm was used as carrier gas. Hydrogen evolved from MWCNTs was probed with gas chromatograph equipped with TCD (thermal conductivity detection method) and the selected capillary column (CARBOXEN 1006PLOT). The temperature scanning range and its rate were set to 280−

* Author to whom correspondence should be addressed. E-mail: jeungku@kaist.ac.kr.
[†] Korea Advanced Institute of Science and Technology.
[‡] Samsung Electronics Co. Ltd.
[§] Samsung Advanced Institute of Technology.

10.1021/jp044727b CCC: $30.25
Published on Web 04/19/2005

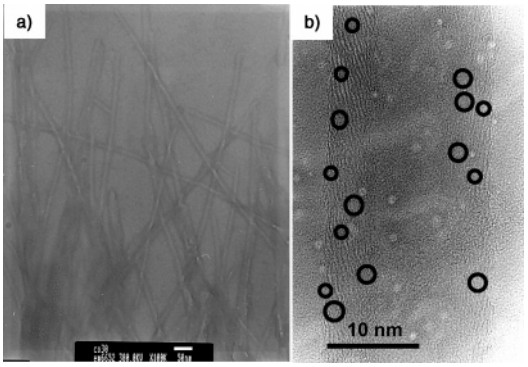

Figure 1. TEM and HRTEM pictures of the MWCNTs grown using $CH_4/H_2/O_2$ reaction gases. The scale bars indicate (a) 50 nm, and (b) 10 nm.

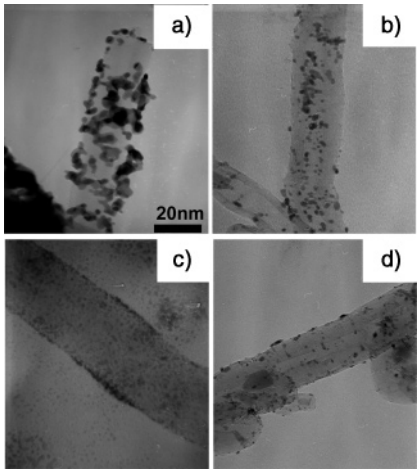

Figure 2. TEM pictures of MWCNTs coated with Ni nanoparticles; the loading amounts are (a) 40 wt %, (b) 13 wt %, (c) 6 wt %, and (d) 3 wt %.

673 K and 1.5−4.5 K/min, respectively. Gas chromatograph separated one gas species and ensured that only hydrogen is involved in desorption peak. The reference hydrogen peak enabled the accurate determination of evolved hydrogen amount by integration of the peak area. The activation energies for desorption was estimated using Kissinger's method.[17] To analyze chemical bonds in CNTs before and after hydrogenation, Fourier transform infrared (FTIR) studies of MWCNTs were performed on the spectrometer with an MCT-b detector. The MWCNTs samples were prepared by mixing 0.001 g MWCNTs with 0.1 g KBr powder and pressing into transparent pellet. Approximately 32 scans were collected.

As shown in Figure 1a and b, the pristine MWCNTs grown using $CH_4/H_2/O_2$ reaction gas have the aligned structure. The nanoholes in MWCNTs were not the closed structures such as bamboo type. HRTEM images of tube end parts reveal that most tubes are open state, and the defective interlayer slits (circles in Figure 1b) with the size of 1 nm were found. They may form because of insufficient graphitization in oxygen plasma atmosphere, which results in an incompact aggregate of graphite nanocrystallite or imperfect stacking of grapheme layers. These nanopores are similar with those found by Hou et al.[18] and Gao et al.[19] Through a detailed analysis of numerous different TEM images, the outer and inner diameters were estimated to be about 20 and 8 nm, respectively.

Figure 2a and d shows the morphologies of the MWCNTs after Ni nanoparticles impregnation by wetting in nitrate solutions of various concentrations. The loading amount of metal

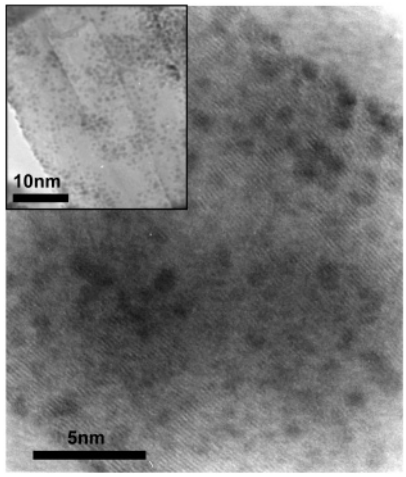

Figure 3. HRTEM picture of MWCNTs containing 6 wt % Ni nanoparticles; several dark spots on the graphite wall are identified as the dispersed metallic Ni particles.

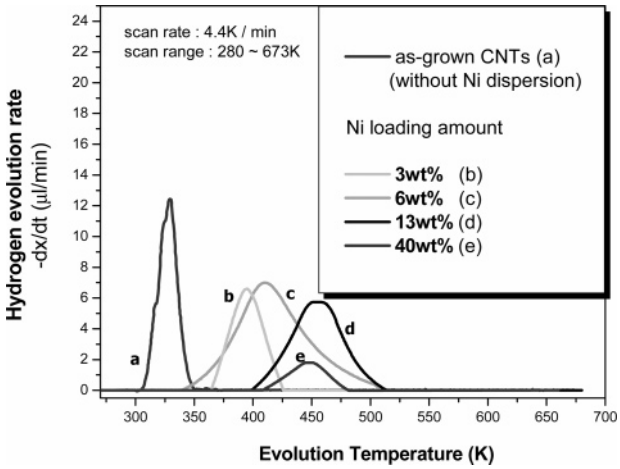

Figure 4. Comparison of hydrogen thermal desorption spectra of nanoparticle-dispersed MWCNTs (3, 6, 13, and 40 wt % Ni loading).

particles varied depending on the concentration of precursor solution.[14] As concentration increases from 5 to 73 mM, more metallic Ni particles were coated on MWCNTs surface between 3 and 40 wt %. When 40 and 13 wt % Ni loaded, the agglomerated Ni of ∼10 nm was scattered on the whole carbon surfaces. MWCNTs covered with 6 wt % Ni particles show well-dispersed Ni particles as small as ∼1.2 nm, and only some Ni islands are observed on carbon surface after less than 3 wt % loading.

As shown in Figure 3, in closer observation of MWCNTs containing 6 wt % Ni, the black spots of Ni particles were distributed widely over CNTs surface.

Figure 4 displays the TDS for hydrogen desorption from Ni nanoparticle-dispersed MWCNTs.

For Ni nanoparticle-dispersed MWCNTs, hydrogen evolution was observed to occur at a slightly higher temperature between 330 and 520 K than that of MWCNTs without Ni dispersion. The hydrogen evolution amounts of MWCNTs with Ni loading of 3, 6, 13, and 40 wt % were 1.2, 2.8, 1.8, and 0.4 wt %, respectively. It is noteworthy that 6 wt % of Ni dispersed MWCNTs released approximately 2.8 wt % of hydrogen, which was 0.9 wt % higher than that of hydrogen evolved from MWCNTs without Ni dispersion. The large amount of hydrogen released near ambient temperature for MWCNTs without Ni dispersion may be due to the nanopores with ∼1 nm diameters

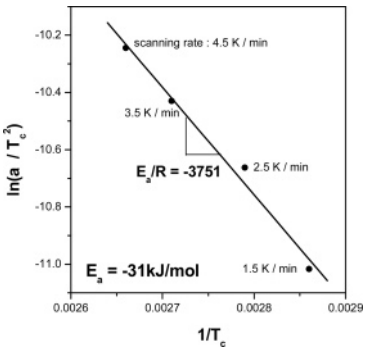

Figure 5. Hydrogen desorption energy of MWCNTs with Ni nanoparticles (T_C = desorption peak temperature, α = scanning rate, R = gas constant).

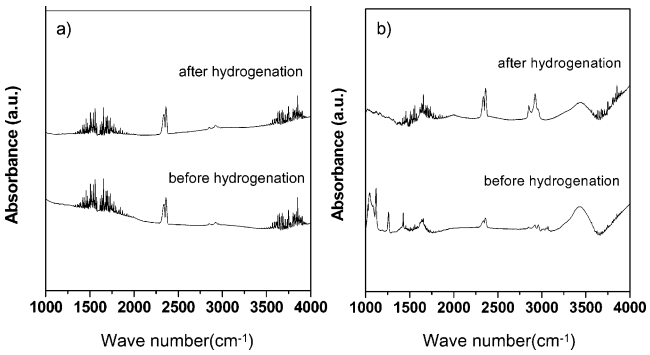

Figure 6. FTIR spectra before (below one) and after (above one) hydrogenation of (a) pristine MWCNTS and (b) Ni nanoparticle-dispersed MWCNTs. Inset is the magnified spectra in the range of 2600−3200 cm^{-1}.

(circles in Figure 1b) generated in oxygen plasma atmosphere, according to the reports of H. Gao et al.[19] and P. X. Hou et al.[18]

In cases of Ni dispersed MWCNTs, hydrogen desorption temperatures were increased about 60−120 K compared with MWCNTs without Ni dispersion, which indicated that the adsorbed hydrogen molecules in the presence of highly dissociative catalysts are more stable. For 6 wt % of Ni dispersed MWCNTs, the hydrogen desorption activation energy was determined by Kissinger's method.[17] Generally, the gas evolution temperature (T_C) changes with variation of temperature scanning rate (α = 1.5−4.5K/min), and Kissigner's plot was shown in Figure 5. The desorption activation energy is measured to be ~31 kJ/mol·H_2, which is higher than the estimates in pure SWNTs.[2] The higher desorption activation energy implies that the hydrogen storage mechanism is closely associated with chemical interaction between hydrogen and carbon.

Figure 6a and b shows FTIR spectra of MWCNTs with and without Ni nanoparticle dispersion, respectively. All of them have the distinct absorption bands corresponding to sp^2 C−C and C═C (aromatic and olefinic) stretching vibrations in the range of 1395−1620 cm^{-1}.[20] As shown in Figure 6a, in as-produced MWCNTs, the weak absorbance between 2850 and 3300 cm^{-1} consistent with C−H_n stretching vibration is observed and remains unchanged after hydrogenation. On the contrary, the Ni particle-dispersed MWCNTs storing hydrogen show prominent increase of C−H_n stretching vibration peak compared to the spectrum before hydrogen absorption (Figure 6b), which further supports that Ni nanoparticles play an important role in dissociative adsorption of hydrogen on carbon atoms. Figure 6b shows the strong absorbance band around 2915 cm^{-1} and the relatively weak band at 2854 cm^{-1}. Some matching C−H bond configurations are indicated in Table 1.[21]

TABLE 1: Various C−H Stretching Vibration Bands[a]

configuration	predicted frequency (cm^{-1})
sp^2 CH_2 (olefinic)	3020
sp^2 CH (olefinic)	3000
sp^3 CH_3 (asymmetric)	2960
sp^2 CH_2 (olefinic)	2950
sp^3 CH_2 (asymmetric)	2925
sp^3 CH	2915
sp^3 CH_3 (symmetric)	2870
sp^3 CH_2 (symmetric)	2855

[a] Reference 21.

The observed frequency around 2915 cm^{-1} could be assigned to an sp^3 CH stretch mode, which implies that the sp^2 nature of the nanotube wall partially changes into single hydrogen-bonded sp^3 configuration upon H_2 adsorption. These findings are consistent with the theoretically expected tendency for sp^2−sp^3 rehybridization by Tada et al.[22] Another absorbance around 2854 cm^{-1} corresponds to the dihydride sp^3 CH_2 bond state, and it is considered that some hydrogen atoms preferentially adsorb on dangling bonds of amorphous carbon or nanotube edge rather than graphite surface in the form of tetrahedral dihydride configuration.

From Figure 4, it should be noted that the desorption temperatures slightly increased with the increase of the amount of Ni dispersion. This result indicates that Ni nanoparticles play an important role of hydrogen adsorption on carbon nanotube surface as well as hydrogen dissociation. Our theoretical prediction of the heat of change for hydrogen adsorption on the CNT using the B3LYP[23]/6-31+G(d,p)[24] density functional theory method shows that each Ni dispersed on the CNT can also accommodate up to five hydrogen molecules. On the other hand, to clarify the role of Ni nanoparticles, we are in the process of further experiments.

A reversibility of hydrogen absorption and desorption was also tested. The hydrogen desorption amount is maintained in the similar temperature range (320−520 K). As a result, the chemical H adsorption and desorption using dispersed Ni nanocatalysts could be considered as a potential reversible process. The MWCNTs used in this experiment show the aligned open structure so that Ni nanocatalysts probably exist both inside and outside of CNTs. Ni is believed to act as an active hydrogen dissociation catalyst and has an important role as the site for hydrogen adsorption on the surfaces of MWCNTs.

When Ni nanoparticles are impregnated on MWCNTs surfaces homogeneously, a high hydrogen uptake up to 2.8 wt % has been achieved under a moderate temperature and pressure condition. As expected hypothetically, Ni catalyst is determined to allow hydrogen molecules to dissociate and adsorb on carbon structures with the higher heat of change. In the detailed analysis on the adsorbed hydrogen configurations using FTIR, the strong monohydride and weak dihydride sp^3 bonding were observed. Accordingly, it is proven that the sp^3 transition occurs clearly while the dissociated hydrogen interacts with the carbon atom on the tube wall. In addition, the dangling bonds of amorphous carbon and graphite edges are considered as another stable hydrogen storage site. Consequently, the chemical hydrogen adsorption and desorption process using nanosized transition-metal catalyst could be suggested as one of the prospective hydrogen storage methods in multiwalled carbon nanotubes.

Acknowledgment. This project was supported by Korea Ministry of Science and Technology (Grant No. M10214000099) and interdisciplinary research program of KOSEF.

References and Notes

(1) Iijima, S. *Nature* **1991**, *354*, 56.
(2) Dillon, A. C.; Johns, K. M.; Bekkedahl, T. A.; Klang, C. H.; Bethune, D. S.; Heben, M. J. *Nature* **1997**, *386*, 377.
(3) Chen, Y.; Shaw, D. T.; Bai, X. D.; Wang, E. G.; Lund, C.; Lu, W. M.; Chung, D. D. L. *Appl. Phys. Lett.* **2001**, *78*, 2128.
(4) Zuttel, A.; Nutzenadel, Ch.; Mauron, Ph.; Emmenegger, Ch.; Sudan, P.; Schlapbach, L.; Weidenkaff, A.; Kiyobayashi, T. *Proc. Int. Symp. Met.*−*Hydrogen Syst.* **2000**, 148.
(5) Stan, G.; Cole, M. W. *Low Temp. Phys.* **1998**, *100* (1/2), 539.
(6) Williams, K. A.; Eklund, P. C. *Chem. Phys. Lett.* **2000**, *320*, 352.
(7) Ye, Y.; Ahn, C. C.; Witham, C.; Fultz, B.; Liu, J.; Rinzler, A. G.; Colbert, D.; Smith, K. A.; Smalley, R. E. *Appl. Phys. Lett.* **1999**, *74*, 2307.
(8) Jin, C. M. *J. Phys. Chem.* **1994**, *98*, 4215.
(9) Chan, S. P.; Chen, G.; Gong, X. G.; Liu, Z. F. *Phys. Rev. Lett.* **2001**, *87*, 205502.
(10) Bai, X. D.; Zhong, D.; Zhang, G. Y.; Ma, X. C.; Liu, S.; Wang, E. G. *Appl. Phys. Lett.* **2001**, *79*, 1552.
(11) Chen, P.; Wu, X.; Lin, J.; Tan, K. L. *Science* **1999**, *285*, 91.
(12) Yang, R. T. *Carbon* **2000**, *38*, 623.
(13) Che, G.; Lakshmi, B. B.; Fisher, E. R.; Martin, C. R. *Nature* **1998**, *393*, 346.
(14) Joo, S. H.; Choi, S. J.; Oh, I.; Kwak, J.; Liu, Z.; Terasaki, O.; Ryoo, R. *Nature* **2001**, *412*, 169.
(15) Lee, H.; Kang, Y. S.; Lee, J. Y. *J. Alloy Comput.* **2002**, *330*, 569.
(16) Lee, H.; Kang, Y. S.; Kim, S. H.; Lee, J. Y. *Appl. Phys. Lett.* **2002**, *80*, 577.
(17) Kissinger, H. E. *Anal. Chem.* **1957**, *29*, 1702.
(18) Hou, P. X.; Xu, S. T.; Ying, Z.; Yang, Q. H.; Liu, C.; Cheng, H. M. *Carbon* **2003**, *41*, 2471.
(19) Gao, H.; Wu, X. D.; Li, J. T.; Wu, J. T.; Lin, J. Y.; Wu, K.; Xu, D. S. *Appl. Phys. Lett.* **2003**, *83*, 3389.
(20) McKenzie, D. R.; McPhedran, R. C.; Savvdes, N.; Botten, L. C. *Philos. Mag.* **1983**, *B48*, 341.
(21) Dischler, B.; Bubenzer, A.; Koidl, P. *Solid State Commun.* **1983**, *348*, 105.
(22) Tada, K.; Furuya, S.; Watanabe, K. *Phys. Rev. B* **2001**, *63*, 155405.
(23) Becke, A. D. *J. Chem. Phys*. **1993**, *98*, 5648.
(24) Frisch, M.; Pople, J. A.; Bikkley, J. S. *J. Chem. Phys.* **1984**, *80*, 3265.